Carbon and nitrogen uptake and export in the equatorial Pacific at 150øW: Evidence of an efficient regenerated production cycle

Patrick Raimbault, Gerd Slawyk, Benyahia Boudjellal, Christine Coatanoan, Pascal Conan, Bernard Coste, Nicole Garcia, Thierry Moutin, Mireille Pujo-Pay

JOURNAL OF GEOPHYSICAL RESEARCH, VOL. 104, NO. C2, PAGES 3341–3356, FEBRUARY 15, 1999

Carbon and nitrogen uptake and export in the equatorial Pacific at 150°W: Evidence of an efficient regenerated production cycle

Patrick Raimbault, Gerd Slawyk, Benyahia Boudjellal,[1] Christine Coatanoan, Pascal Conan, Bernard Coste, Nicole Garcia, Thierry Moutin, and Mireille Pujo-Pay

Laboratoire d'Océanographie et de Biogéochimie (UMR CNRS 6535), Centre d'Océanologie de Marseille, Campus de Luminy, Marseille Cedex, France

Abstract. Biomass, inorganic carbon and nitrogen uptake, ammonium regeneration, nitrification, and vertical flux of particulate matter were measured in the equatorial Pacific at 21 daily productivity stations occupied on a meridional transect (150°W) between 1°N and 16°S. Three areas could be distinguished along the transect: (1) the equatorial area between 1°N and 6°S, where nitrate concentrations were typically eutrophic, reaching up to 3 μg-at L^{-1} in surface waters; (2) an intermediate mesotrophic area between 6° and 10°S, where surface nitrate concentrations decreased from 1 μg-at L^{-1} to zero; and (3) the oligotrophic area beyond 10°S, characterized by warm and nitrate poor waters. Although nitrate was the main form of inorganic nitrogen available for phytoplankton growth (70%–100% of total), its uptake was severely retarded in the equatorial sector. This lack of nitrate depletion in the equatorial sector between 0 and 6°S may in part result from the important ammonium supply (100 ng-at L^{-1} d^{-1}) which could sustain up to 85% of total inorganic nitrogen (nitrate + ammonium) utilization by phytoplankton. In addition, regenerated production also resulted from in situ nitrification (20–80 ng-atN L^{-1} d^{-1}) which can fuel 20%–100% of the nitrate uptake. Sinking particles represented <10% of total carbon fixation and ~10%–50% of new production in terms of carbon and nitrogen. From these discrepancies it was suggested that (1) new production rates were overestimated because of the high level of nitrification that provided "regenerated nitrate" and (2) advection of dissolved organic carbon and nitrogen played an important role in export. The specific hydrodynamical circulation, a conveyor belt generated by upwelling at the equator and downwelling some degrees south, associated with biological in situ remineralization of ammonium and nitrate as well, appeared to be a very efficient system for recycling inorganic nitrogen in the euphotic layer and thus for supporting the high regenerated production levels. On the other hand, the high nitrate/silicate ratios (>1.5) observed in the upwelling waters seemed to indicate that silicate is not efficiently recycled in this specific circulation system because of its low regeneration rate as well as its sink via rapidly sedimenting diatoms cell walls; this may be also true for iron. This reinforces the idea of Si and/or Fe limitation which was put forward earlier to explain low new production levels in the equatorial Pacific.

1. Introduction

New production, defined as the fraction of primary production driven by the input of new nutrients (usually nitrate) into the euphotic zone [*Dugdale and Goering*, 1967], and export production, defined as the fraction of primary production exported as particles (carbon and nitrogen) [*Eppley and Peterson*, 1979], are important variables that characterize the efficiency of carbon and nitrogen cycling and particle export from the biological food web in the ocean. These fractions of photosynthetic production play a role in the transport of atmospheric carbon dioxide to the ocean interior, and their quantification is needed to estimate the ability of the ocean to act as a sink for carbon dioxide. New production, and consequently carbon export by biological processes, is enhanced in regions of the ocean where turbulent mixing or upwelling enrich surface water with nutrients. Because of persistent upwelling, the equatorial Pacific includes areas of high productivity that may contribute significantly to high new production and thus to the global flux of carbon. Using data on the vertical flux of nitrate into the photic zone, new production in terms of carbon, and the proportion of new to total production (f ratio) [*Eppley and Peterson*, 1979], *Chavez and Barber* [1987] estimated that the central and eastern Pacific contributed 18%–56% of global new production. Recent investigations using direct measurements of new production with the ^{15}N tracer [*Dugdale et al.*, 1992; *Peña et al.*, 1992b; *McCarthy et al.*, 1996] showed a lower contribution (5%–17%). The lack of agreement between the latter observation and the former estimation arises from the high f ratio (0.4) used by *Chavez and Barber* [1987]. Direct measurements led to lower values of f (0.1–0.3) [*Dugdale et al.*,

[1]Now at Institut des Sciences de la Mer et de l'Aménagement du Littoral, Staoueli, Algeria.

Paper number 1998JC900004.
0148-0227/99/1998JC900004$09.00

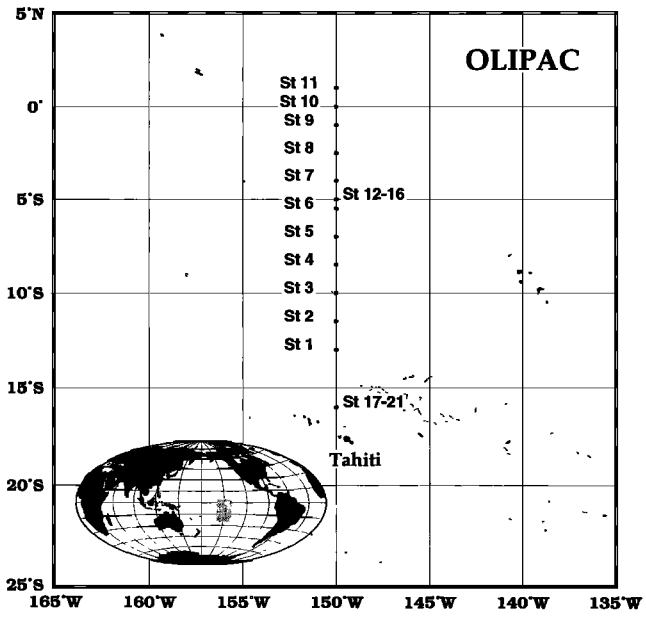

Figure 1. Study area with station locations.

1992; *McCarthy et al.*, 1996] indicating that although nitrate is the dominant form of inorganic nitrogen in the environment, most primary production is fueled by regenerated forms of nitrogen, namely, ammonium. In fact, nitrate supplied by equatorial upwelling is not immediately consumed but horizontally advected westward at ~40 cm s^{-1} and poleward according to the zonal current system driven at variable rates by easterly winds [*Kessler and McPhaden*, 1995]. Within 5° on either side of the equator, convergence results in downwelling and recirculation of the surface water back toward the equator. The freshly upwelled surface water at the equator would be expected to be enriched in macronutrients and micronutrients, and increased availability of light should allow the resident phytoplankton to take advantage of these nutrients. As this water is advected from the equator, it would be expected to mature with chlorophyll biomass increasing if there is a growth-grazing imbalance.

However, despite high macronutrient concentrations (nitrate 3 μg-at L^{-1}) [*Chavez and Barber*, 1987; *Murray et al.*, 1994] and an adequate input of solar radiation, phytoplankton pigment biomass is considerably lower than expected [*Thomas*, 1979]. The equatorial Pacific thus has been described as a high-nutrient/low-chlorophyll (HNLC) area [*Minas et al.*, 1986]. Several hypotheses have been evoked to explain this enigmatic feature, including physical processes [*Thomas*, 1972], initial nitrate concentration below some "physiological threshold" necessary to induce maximal uptake rates [*Wilkerson and Dugdale*, 1992], inhibition of nitrate uptake by ammonium [*Murray et al.*, 1989], grazing pressure which reduces biomass and in turn reduces absolute uptake rates [*Walsh*, 1974], and iron limitation [*Martin*, 1990]. As nitrate uptake is severely retarded, pCO_2 in surface waters remains elevated, and thus the sea surface becomes a net source of CO_2 to the atmosphere. Therefore the equatorial Pacific may be the largest marine source of CO_2 to the atmosphere [*Tans et al.*, 1990]. Despite its large area and the potential importance in the CO_2 exchange with the atmosphere through biological processes, there are relatively few data available on biological processes in the equatorial Pacific. Especially scarce are the direct measurements of new and regenerated production required for estimates of the *f* ratio as well as direct measurements of export production in the upper ocean in terms of sinking rates of particles. Prior to the present study the only detailed sections concerning new and regenerated production appear to be those of *Wilkerson and Dugdale* [1992] and of *McCarthy et al.* [1996]. However, measurements of inorganic nitrogen regeneration have not been done so far. Particle export using sediment traps has been mostly studied in deep waters. Corresponding measurements in the upper layer are sparse, although much of the particle cycle takes place in this layer. Although a positive correlation between surface primary productivity and the downward flux of particulate materials is well established in a qualitative sense [*Suess*, 1980; *Deuser et al.*, 1981], the quantitative nature of this relationship remains unclear.

The present investigation, conducted during the Oligotrophie en Pacifique (OLIPAC) cruise in November 1994, was undertaken as a part of the Joint Global Ocean Flux Study (JGOFS) program which is focused on the study of new and total production, the factors controlling these biological processes, and the export of photosynthesized materials to the deep ocean and sediments. This cruise provided the opportunity to measure directly inorganic carbon and nitrogen (nitrate and ammonium) uptake and ammonium regeneration using isotopic tracers (^{14}C and ^{15}N) as well as export production in terms of vertical particle flux using floating sediment traps on a meridional track along 150°W from 16°S to 1°N. This work also includes observations on nutrients and biomass (chlorophyll, carbon, and nitrogen).

2. Materials and Methods

This work was performed aboard the R/V *L'Atalante* during the OLIPAC cruise which formed a part of the JGOFS-France project. Hydrological measurements and biological experiments were conducted over the period November 3 to November 30 in the equatorial Pacific at 21 stations occupied along a transect at 150°W between 16°S and 1°N (Figure 1). Nutrients, particulate organic nitrogen (PON), particulate organic carbon (POC), chlorophyll *a*, ^{15}N and ^{14}C uptake rates, and sinking rates of carbon and nitrogen in particles were daily measured within the 0–200 m layer. The 1% light penetration depth (1% LPD) was calculated from a profile of photosynthetically active radiation (PAR) performed about noon using a biospheric instrument (PNF-300). Hydrographic measurements were done with a conductivity-temperature-oxygen-depth profiling system (CTOD Seabird, model SBE 911). Simultaneous in vivo chlorophyll fluorescence was measured by a SeaTech fluorometer (model SN 38S). Continuous multiparametric profiles obtained during the 0–200 m downcasts were examined to select 12 sampling depths for the upcasts in order to always encompass the chlorophyll *a* maximum. Samples were obtained with 12 L Niskin bottles with silicone rubber closures and tubing that had been carefully checked to avoid introducing toxic metals during sampling. Samples for nitrate + nitrite, silicate, and phosphate were collected in polyethylene flasks and were analyzed immediately after sampling on a Technicon Auto-Analyzer^{R} according to *Tréguer and LeCorre* [1975]. Samples for POC (3 L), PON (250 mL), and chlorophyll *a* (250 mL) were filtered using precombusted GF/F glass-fiber filters. Chlorophyll *a* concentration was determined by fluorimetry using

the methanol extraction procedure as described by *Raimbault et al.* [1988]. The filters for POC were kept dry until later analysis in the lab with a carbon-hydrogen-nitrogen (CHN) LECO 800 elemental analyzer. The filters were not treated to remove carbonates. Filters for PON were immediately treated on board using a persulfate wet-oxidation method [*Pujo-Pay and Raimbault*, 1994]. For dissolved organic nitrogen (DON), unfiltered samples were collected in 50 mL Pyrex bottles. Total nitrogen (TN = inorganic + particulate and dissolved organic nitrogen) were measured on board by the wet-oxidation procedure using the same reagent as for PON. DON concentrations were calculated as TN minus dissolved inorganic nitrogen (DIN) and PON.

For productivity measurements, samples collected before sunrise with Niskin bottles were poured into acid-cleaned polycarbonate (PC) bottles (1.2 or 2.4 L for ^{15}N experiments and 250 mL for ^{14}C experiments). The bottles were rinsed after use with 10% HCl, then with distilled water from a Milli Q ion exchange unit. Ambient nitrate, nitrite, and ammonium were immediately measured by directly pumping with the Technicon^R AutoAnalyser in the incubation bottles. Ammonium concentrations were determined according to *Tréguer and Le Corre* [1975] with a lower detection limit of 100 ng-at L^{-1}. Nitrate and nitrite concentrations in the nanomolar range (lower detection limit = 3 ng-at L^{-1}) were obtained from a sensitive method according to *Raimbault et al.* [1990]. Nitrogen 15–tracer additions as $K^{15}NO_3$ and $^{15}NH_4Cl$ (99 at.% ^{15}N) were usually 10%–20% of the ambient concentration. However, in nutrient impoverished oligotrophic waters, minimal additions of ^{15}N (42 ng-at L^{-1}) resulted in substrate enrichments of 50%–100%. It should be noted that these ^{15}N additions above tracer amount could significantly alter the nitrogen environment of phytoplankton and thus the measured uptake rates [*Allen et al.*, 1996; *Harrison et al.*, 1996]. The initial nitrate, nitrite, and ammonium concentrations were always verified after the tracer addition (T_0 concentrations). The PC bottles were then incubated under in situ conditions. The in situ array was typically launched at dawn and recovered after sunset (i.e., 12 hours incubation period) during the first 11 stations along the transect. During two repeating stations at 5° and 16°S incubation lasted 24 hours. Following incubation, concentrations of DIN were again measured directly in the PC flasks. The samples were then filtered onto 25 mm precombusted GF/F filters using low vacuum (<100 mm Hg). Subsequent to filtration, the filters were dried at 60°C and stored with dessicant. A 300 mL GF/F filtrate was again filtered on a 0.2 μm Anopore membrane and directly collected in a 500 mL Pyrex bottle (Duran Schott). These <0.2 μm filtrates were poisoned with $HgCl_2$ (20 μg mL^{-1}) and kept in the dark at ambient temperature until laboratory processing to determine ^{15}N enrichment in the DIN and DON pool according to the method described by *Slawyk and Raimbault* [1995]. In this procedure all DIN and DON forms were removed from the filtrate as ammonium sulfate by successive diffusion and collection on glass-fiber filters appropriate for the mass spectrometric assay. The first diffusion step allowed to obtain the final ^{15}N enrichment of the DIN pool and thus to estimate isotope dilution of the tracer. The second diffusion following a wet oxidation of DON was done to estimate the ^{15}N abundance in the DON pool. This procedure was improved to estimate nitrification (oxidation of ammonium to nitrate) by measuring the ^{15}N enrichment in the nitrate pool from some filtrates of ammonium uptake experiments. To do this, Devarda alloy was added (300 mg) to reduce nitrate to ammonium after the initial ^{15}N-labeled ammonium had been removed (first diffusion step). The liberated ammonium derived from the reduction step was then trapped on a filter by a further diffusion step. All filters containing particles and trapped ammonium were analyzed for ^{15}N content using a continuous-flow method (Europa Scientific in which Dumas combustion (Roboprep-CN) is linked on-line to a triple collector mass spectrometer (tracer-mass) via a capillary interface based on the design of *Preston and Owens* [1983]. Mass-spectrometric signals were used to calculate ^{15}N abundance in PON, DIN, and DON. Total beam (mass 28, 29, and 30) intensities were used to estimate PON (μg-at L^{-1}). The transport rate of nitrogen from the DIN pool to the PON pool; that is, the net DIN uptake rate (ρDIN, in ng-at L^{-1} h^{-1}) was computed from an equation based on a value for final PON concentration [*Dugdale and Wilkerson*, 1986]:

$$\rho\text{DIN} = [(R_{\text{PON}}/R_{\text{DIN}})T][\text{PON}] \quad (1)$$

where R_{PON} and R_{DIN} are the ^{15}N atom percent excess enrichment in the PON and DIN pool, respectively. [PON] corresponds to the final PON concentration. T is the incubation period in hours. Ammonium regeneration was estimated using the initial and final ^{15}N-NH_4 enrichment according to *Glibert et al.* [1982]. Ammonium uptake rates were corrected for isotopic dilution by using for R_{DIN} in (1) the mean value between initial and final enrichment in the ammonium pool ($\bar{R}_{\text{NH}_4}$). No significant isotope dilution was detected for nitrate, so that R_{DIN} for nitrate in (1) corresponds to the initial ^{15}N atom percent excess enrichment in the nitrate pool (R_{NO_3}). Nitrification rates (ρnit, in ng-at L^{-1} h^{-1}) were calculated as follows:

$$\rho\text{nit} = [(R_{\text{NO}_3}/R_{\text{NH}_4})T][\text{NO}_3] \quad (2)$$

where R_{NO_3} and $[\text{NO}_3]$ are the ^{15}N atom percent excess enrichment and the final concentration (initial + carrier addition) of nitrate measured by mass spectrometry. $\bar{R}_{\text{NH}_4}$ is the mean ^{15}N enrichment of ammonium.

The f ratio was calculated from

$$f = \rho\text{NO}_3/(\rho\text{NO}_3 + \rho\text{NH}_4) \quad (3)$$

No corrections were made for the possible contribution of urea since urea uptake was not measured.

Carbon fixation was measured in four 250 mL aliquots collected in PC bottles and incubated at the same depth and during the same time interval as for the ^{15}N uptake experiments. Each incubation bottle was spiked with 20 μCi of $NaH^{14}CO_3$ to initiate incubation. An extra sample was inoculated with ^{14}C and immediately filtered to determine abiotic fixation. After incubation, samples were filtered onto Whatman GF/F filters at <100 mm Hg, and the filters were placed in scintillation vials. To chase inorganic ^{14}C on the filters, 250 μL of HCl 0.5 N were added, and after 6–12 hours the filters were counted in 10 mL Aquasol in a liquid scintillation counter. All fixation rates were corrected for dark fixation determined at each depth using a dark bottle incubated under the same conditions as light bottles.

Some ^{15}N and ^{14}C samples were filtered on 0.2 μm Anopore membranes. While Anopore 0.2 μm membranes retained much more particulate nitrogen (up to 40% in low-PON waters) than GF/F filters (Figure 2a), the ^{15}N uptake rates obtained from these former membranes compared quite well with those obtained from GF/F filters (Figure 2b), indicating that

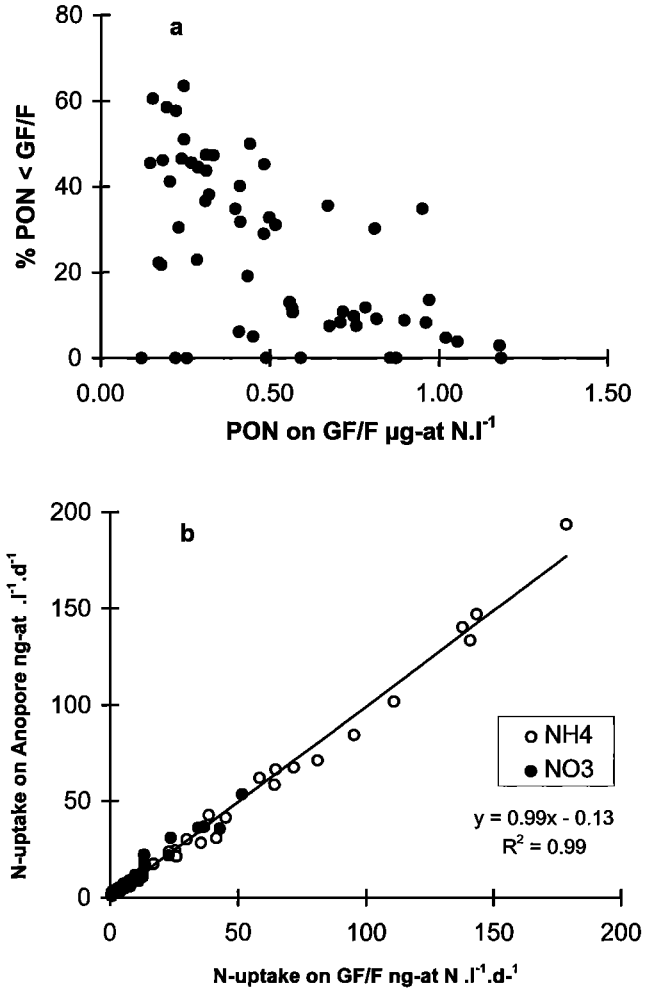

Figure 2. (a) Percentage of particulate organic nitrogen (PON) passing through GF/F filters and retained by 0.2 μm Anopore membranes (%PON < GF/F) versus PON retained by GF/F filters. (b) Efficiency of the GF/F filters compared to 0.2 μm Anopore membranes to measure inorganic nitrogen uptake.

glass-fiber filters were fully adequate for ^{15}N uptake measurements. Ten identical comparisons performed with the ^{14}C tracer gave similar results with no significant underestimation of primary production rates when using GF/F filters instead of Anopore 0.2 μm membranes (C uptake on GF/F = 95.4 ± 16% ^{14}C uptake on Anopore). Downward fluxes of particulate matter (PM) were measured in free-floating sediment traps (PPS4) deployed at a depth of 200 m. These cylindrical sediment traps have a mouth area of 0.05 m^2 and a height of 1.20 m. In our system the trap material was concentrated in a polyvinyl receptacle (10 cm height) placed at the bottom of the trap. The flasks were isolated from further inputs during launching and recovery by a valve that was activated by an electronic device with a timer. The collected flask was filled with filtered seawater containing no preservatives. In order to avoid microbial degradation of the PM to a maximum, traps were deployed during short time intervals (10 hours along the transect and 22 hours at 5° and 16°S) in parallel with the in situ ^{14}C and ^{15}N incubations. Estimates of the total particle flux were made gravimetrically. PM was filtered onto tared 25 mm precombusted GF/F filters immediately after recovery. Swimmers were scarce but when present were immediately removed from the filter using forceps. To eliminate residual salt water, filters were given three brief rinses with deionized water. They were then dried at 60°C and placed in a dessicator with silica gel and stored dry until they could be reweighed at the laboratory. After weighing, filters were analyzed with a CHN LECO 800 to determine the carbon and nitrogen content of the PM.

To facilitate comparisons with data from literature, all sediment fluxes as well as production rates were converted in daily rates. For heterotrophic processes (ammonium regeneration and nitrification) and sediment flux we assume no significant influence of the photoperiod; hourly rates were therefore multiplied by 24. For ammonium and nitrate uptake, some direct comparisons between 12 and 24 hour incubations were performed. During the transect, where in situ incubations were stopped at sunset, some subsamples were placed in a deck incubator for the night period before filtration (24 hours for total incubation). While nitrate was not taken up during the night period (Figure 3a), a significant ammonium uptake occurred (Figure 3b). According to these results, ammonium uptake rates obtained from 12 hour incubations (stations 1–11) were multiplied by a factor of 1.3 to compute daily rates. For ^{14}C fixation, such comparative experiments have not been performed, and we assume that dark fixation of carbon did not occur. As for nitrate experiments, the daily rates were estimated from 12 hour rates.

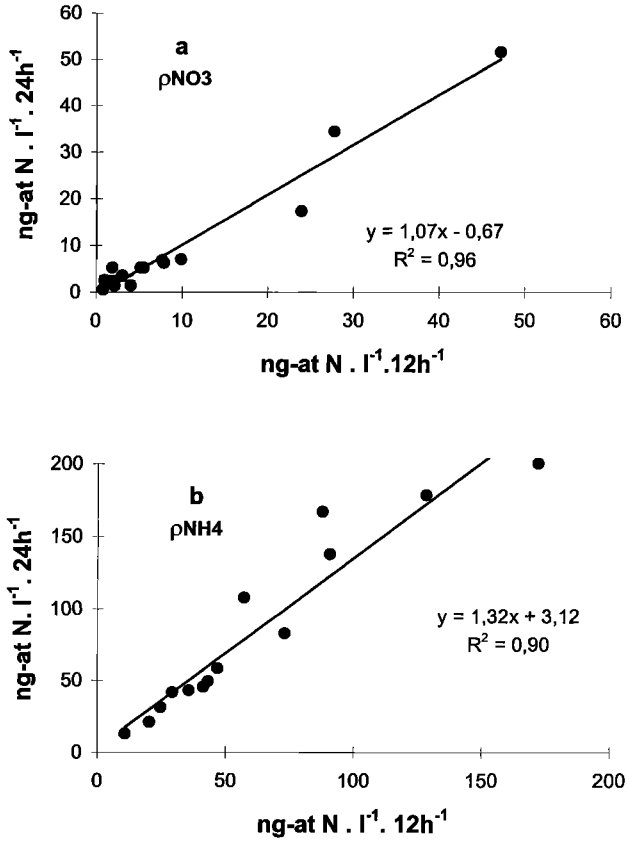

Figure 3. Comparison between 24 hour light-dark and 12 hour light incubations from nitrate and ammonium uptake experiments.

3. Results

3.1. Hydrography, Nutrient, and Biomass Distribution

Data shown throughout the paper are limited to the 0–200 m water column. The south-north distributions of temperature, salinity, nutrients, biomass in terms of chlorophyll, POC, and PON are shown in Figures 4 and 5. Surface temperatures (Table 1) were similar to those observed in February 1988 during the WEC88 cruise [*Carr et al.*, 1992] and in February 1992 during the first Eqpac survey (JGOFS TT07) by *Murray et al.* [1995], but they were a little higher than those noted by *Murray et al.* [1995] in September 1992 (JGOFS-TTO11 cruise), during the typical upwelling season, when surface temperature never reached 28°C and were <25°C at the equator. The contour plot of temperature (Figure 4a) revealed that warm water (>27°C) was always present between surface and ~100 m depth except at 16°S where this isotherm was located near 20 m. The isotherm 28°C surfaced at 16°S, slightly deepened until 100 m at the equator, and again reached the surface at 1°N. Typical upward doming and spreading of isotherms were absent at the equator; this was also observed by *Murray et al.* [1995] in February 1992 during the El Niño event. However, the depth of the mixed layer increased drastically toward the equator from ~40 to 130 m (Table 1). The salinity distribution (Figure 4b) depicted the typical feature with low surface values at the equator (<35.3 practical salinity unit (psu)). The salinity front, generally marked by the outcrop of the 35 psu isohaline at surface near the equator separating northern low-salinity water from southern high-salinity water [*Murray et al.*, 1995; *Carr et al.*, 1992], was not clearly visualized here. The isohaline 35 psu was found at depths >300 m in the southern part of the transect and at ~180 m at the equator. A salinity front was visible between 11° and 12°S where low-salinity water met high-salinity subtropical water. Dense water subducted to form a characteristic high-salinity tongue (>36 psu) located in the upper thermocline between 100 and 200 m and then spreaded equatorward.

Nutrient distributions were generally comparable with those of *Wyrtki and Kilonsky* [1984]. In contrast to temperature, the deep nutrient isolines sunk from north to south; surface nutrients tended to be asymmetrically distributed with high surface values between 1°N and 6°S. The lowest concentrations were found in the mixed layer south of 10°S. The 2 μg-at L^{-1} isoline for nitrate, found at a depth >120 m between 16° and 8°S, rapidly rose to surface at 6°S (Figure 4c). Surface values for nitrate near the equator were lower than those encountered in April 1988 by *Peña et al.* [1992a] at 135°W (>4 μg-at L^{-1}) and in February–March 1988 by *Carr et al.* [1992] at 150°W (>5 μg-at L^{-1}) but were similar to those observed in February 1992 by *Murray et al.* [1995] at 140°W. Nitrate concentrations decreased abruptly at 8°S (<0.5 μg-at L^{-1}) and became <0.1 μg-at L^{-1} between surface and 100 m depth beyond 10°S poleward. At ~7°–10°S, high-nitrate water lay over low-nutrient water as a consequence of downwelling of high-salinity nutrient poor subtropical water. It should be noted that except for this latitude, the vertical distribution of nitrate was relatively uniform throughout the photic zone, even at the equator. The general distribution of phosphate (Figure 4d) was similar to the one of nitrate with highest concentrations (>0.3 μg-at L^{-1}) between 1°N and 6°S. As for nitrate, surface concentrations decreased southward but remained always at significant levels, even at 16°S where they reached 0.15 μg-at L^{-1} between 0 and 100 m. These significant amounts of phosphate in the superficial layer of the subtropical region confirmed previous observations from *Murray et al.* [1995]. The silicate distribution showed the same general pattern as the one for nitrate and phosphate, although concentrations along the transect were less variable than those for nitrate and phosphate (Figure 4e). The equatorial zone was enriched with silicate where concentrations were >1.5 μg-at L^{-1} but never reached 2 μg-at L^{-1} as observed in JGOFS 1992 cruises [*Murray et al.*, 1995]. Surface values decreased to 1 μg-at L^{-1} between 2.5° and 8°S and then remained constant beyond 10°S. Silicate poor waters have been previously noted in March 1988 [*Peña et al.*, 1991]. In spite of the similar general pattern in the geographical distribution of these three important nutrients for new production, differences in concentration changes between them (when moving in the South Pole direction) led to modifications of the N/Si/P molar ratio along the transect (Table 1). The nitrate/phosphate ratio (integrated over 150 m) decreased from 9 to 5 between 1°N and 8°S and remained ~1.5–2 south of 10°S. The molar nitrate/silicate ratio was >1.5 between 1°N and 6°S and <0.7 in the south. In comparison to the Redfield ratio and to the phytoplankton requirement [*Fleming*, 1939], these values indicate a deficit in nitrate and silicate relative to phosphate near the equator (5°N–6°S) and a deficit in nitrate relative to silicate and phosphate in the southern part of the transect. Similar low levels of silicate occurred in 1988 [*Dugdale et al.*, 1992] as a result of a relatively shallow depth of the upwelling source water. It should be noted that nutrient samples from depth >300 m showed typical N/Si/P Redfield ratios (~1/1/16). DON concentrations ranged from 3 to 7 μg-at L^{-1}, with high concentrations generally in the surface water and lowest concentrations below 150 m (Figure 4). Lowest surface concentrations (<5.5 μg-at L^{-1}) were located between 13° and 16°S. A DON maximum (>6.5 μg-at L^{-1}) was found in the upper 100 m between 6° and 10°S, coincident with the sharp decrease in surface nitrate (Figure 6). In the convergence region (11°–13°S), where subtropical water subducted below low-salinity equatorial water (see Figure 4b), surface DON concentrations rapidly decreased from 7 to <5.5 μg-at L^{-1} depicting a sort of DON front.

Concentrations of regenerated nitrogen forms, such as nitrite and ammonium, showed a particular distribution pattern characterized by the presence of two subsurface maxima located south of the equator. Nitrite, a tracer of subtropical water [*Wyrtki and Kilonsky*, 1984] presented a maximum of up to 0.5 μg-at L^{-1} along the thermocline south of the equator (Figure 4g). The ammonium maximum (up to 1 μg-at L^{-1}), centered around 80–100 m, was shallower than the nitrite maximum (Figure 4h). Both maxima were just below the chlorophyll maximum (Figure 4d). These subsurface maxima have also been observed in 1992 at 140°W by *Murray et al.* [1995], while only a small patch of ammonium (0.3 μg-at L^{-1} between 40 and 90 m) was detected at 1°S [*Wilkerson and Dugdale*, 1992]. Concentrations of both regenerated forms were always low or undetectable in the 0–60 m layer except near the equator where they reached 0.20 and 0.10 μg-at L^{-1} for ammonium and nitrite. In the oligotrophic region (around 16°S), ammonium was undetectable all over the water column, while a very narrow nitrite maximum (>0.1 μg-at L^{-1}) was observed near 140 m depth.

Vertical distributions of biomass are shown in Figure 5 in terms of chlorophyll, PON, and POC. Surface chlorophyll concentrations (Figure 5a) increased along the transect from 0.06 at 16°S to 0.35 μg-at L^{-1} at 1°N and were well correlated with

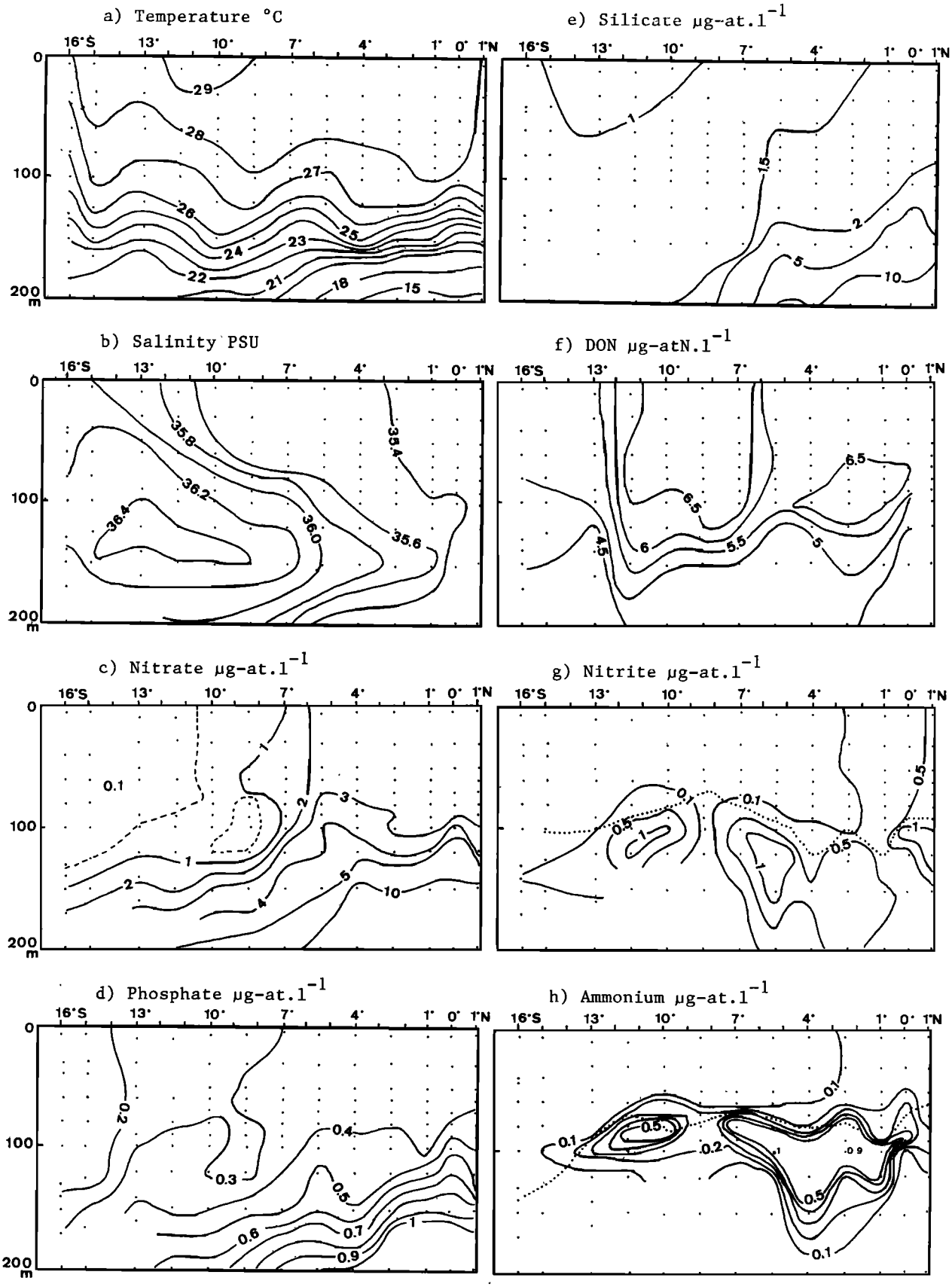

Figure 4. Contour plots of the 150°W transect, depth versus latitude: (a) temperature, (b) salinity, (c) nitrate, (d) phosphate, (e) silicate, (f) dissolved organic nitrogen (DON), (g) nitrite, and (h) ammonium. Dashed line on nitrite and ammonium panels represent depths of chlorophyll maximum and nitrite maximum, respectively. Dashed line on nitrate panel represents the 0.1 µg-at L^{-1} isoline.

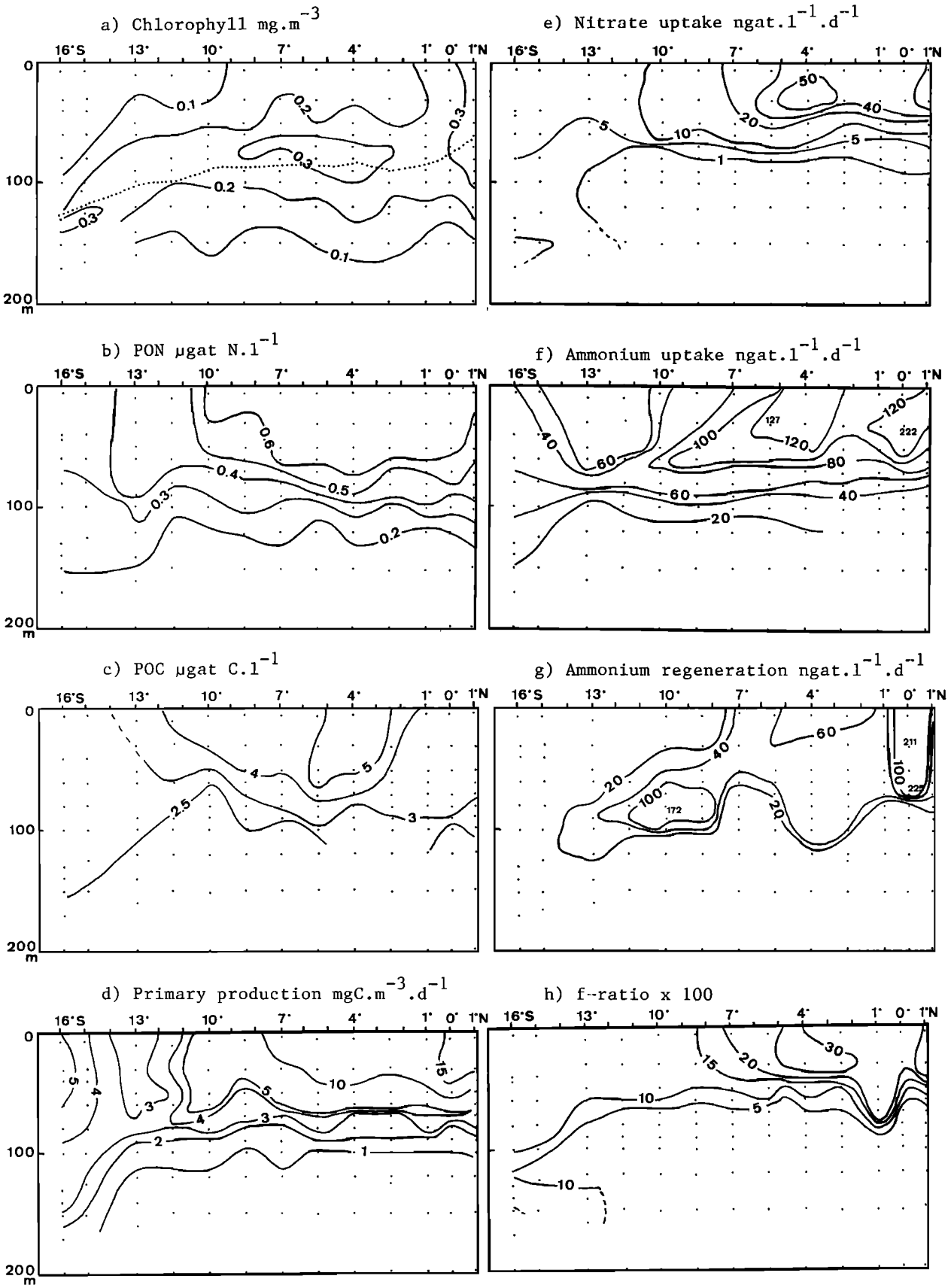

Figure 5. Contour plots of the 150°W transect, depth versus latitude: (a) biomass in terms of chlorophyll *a*, (b) particulate organic nitrogen (PON), (c) particulate organic carbon (POC), (d) primary production, (e) nitrate uptake, (f) ammonium uptake, (g) ammonium regeneration, and (h) *f* ratio (in percent). Dashed line on chlorophyll panel represents depth of 1% light penetration depth (LPD, lower limit of the euphotic zone).

Table 1. Sea Surface Temperature (SST), Mixed Layer Depth, and Integrated Values of Nitrate (Σ Nitrate), Chlorophyll *a* (Σ Chlorophyll), Nitrate/Silicate Ratio (NO_3/Si), Nitrate/Phosphate Ratio (NO_3/PO_4), and Particulate Nitrogen (ΣPON) and Carbon (ΣPOC) for the 1°N–16°S Transect Along 150°W

Station	Latitude °S	SST, °C	Mixed Layer, m	Σ Nitrate, mg-at m^{-2}	Σ Chlorophyll, mg m^{-2}	NO_3/Si	NO_3/PO_4	ΣPON, mg-at m^{-2}	ΣPOC, mg-at m^{-2}
					Equatorial				
11	−1	27.969	70	658.7	40.80	1.68	9.35	56.0	371.2
10	0	28.121	60	685.6	33.30	1.54	9.00	59.1	363.3
9	1	28.178	50	537.0	29.00	1.47	8.15	50.7	374.1
8	2.5	28.443	40	459.0	29.30	2.13	7.82	53.4	391.3
7	4	28.454	40	413.0	35.20	1.69	7.32	57.7	439.6
12	5	28.466	40	557.4	30.15	1.49	8.65	47.0	418.3
13	5.2	28.520	60	482.3	30.80		7.30		430.7
14	5.23	28.525	60	513.3	28.60		7.48	56.1	434.9
15	5.27	28.514	35	498.7	27.80		8.06		
16	5.33	28.550	45	499.9	31.31		7.47		357.0
6	5.5	28.397	20	510.0	30.10	2.01	8.58	57.5	437.3
					Mesotrophic				
5	7	28.764	30	279.7	25.80	1.42	6.01	58.2	352.8
4	8.5	29.006	40	116.6	25.60	0.70	2.70	46.2	347.8
3	10	29.185	20	98.2	23.70	0.56	2.38	49.1	333.7
					Oligotrophic				
2	11.5	29.063	30	91.2	21.80	0.61	2.14	42.1	424.2
1	13	28.817	10	84.4	25.13	0.49	2.00		
17	16	27.851	5	40.3	20.17		1.48	48.5	436.5
18	16	27.889	5	41.2	16.80		1.46	42.8	443.0
19	16	27.923	10	39.5	18.60				
20	16	28.122	10	36.0	19.90	0.26	1.49		
21	16	28.023	5	34.2	24.40				

The mixed layer depth was defined using the continuous profiles obtained with the conductivity-temperature-depth (CTD) probe to precisely determine the beginning of the thermocline (depth where temperature gradient was >0.1°C m^{-1}).

surface concentrations of nitrate ([chlorophyll] = 0.07 [nitrate] + 0.06; r^2 = 0.80; n = 20). All stations showed a typical subsurface chlorophyll maximum (SCM) where concentrations ranged from 0.2 to 0.3 μg L^{-1}, mostly at 70–80 m depth from 2° to almost 12°S and much deeper southward (140 m at 16°S). Within this SCM, concentrations were very homogeneous along the transect, only ranging from 0.27 to 0.33 μg L^{-1}. These levels were similar to those observed in the surface layer near the equator but were 2–6 times higher than surface values in the southern area. While the SCM was generally found just above the 1% LPD, the entire deep chlorophyll maximum (DCM) was below the euphotic zone at 16°S. Because of the relatively high deep chlorophyll concentrations in the subtropical region, the integrated values showed little geographical variation (Table 1). The areal chlorophyll content increased equatorward by a factor of 2 (from 20 to 35 mg m^{-2}) with a steep gradient around 1°S, while surface concentrations changed by a factor of 7. PON and POC concentrations showed little geographical variations (Figures 5b and 5c), and their depth profiles lacked pronounced subsurface maxima as observed for chlorophyll. Surface values were maximum near the equator with 0.65 and 4.5 μg-at L^{-1} for PON and POC, respectively. In the southern region, corresponding values were somewhat lower, 0.4 and 3.0 μg-at L^{-1} for PON and POC, respectively. These latter values, obtained from samples filtered on GF/F membranes, are close to those reported in 1988 by *Eppley et al.* [1992], *Peña et al.* [1991], and *Chavez et al.* [1996] for the same area. However, integrated values (0–150 m, Table 1) did not show obvious latitudinal variations as observed by *Eppley et al.* [1992], who integrated their values over the euphotic zone (1% LPD). Considering that chlorophyll *a* and particulate matter were present below this layer, the choice of the 1% LPD as the limit for their integrations might have led to underestimations of areal contents, especially in the southern oligotrophic region. The fact that POC and PON concentrations decreased slowly with depth in the southern region but changed rather rapidly with depth near the equator may add to this effect. In our case, integrations limited to the euphotic layer (down to the 1% LPD) would have resulted in areal contents of biomass and areal rates of primary productivity (see below) ~15%–20% lower than those obtained from integrations over the 0–150 m column. Moreover, the determination of PON using 0.2 μm Anopore membranes (Figure 2a) has confirmed the earlier observation that the use

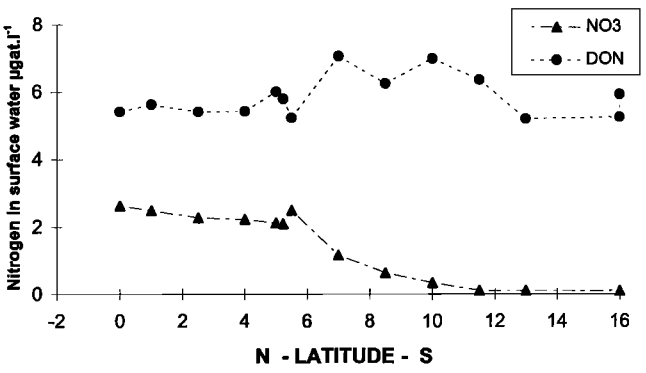

Figure 6. Latitudinal evolution along 150°W of surface concentrations of dissolved organic nitrogen (DON) and nitrate (NO_3).

Table 2. Depth of the Euphotic Zone (1% Light Penetration Depth (LPD)) and Integrated Values of Primary Production (ΣPP), New Production ($\Sigma\rho NO_3$), Regenerated Production ($\Sigma\rho NH_4$), *f* Ratio (Σ Ratio), and New Production in Terms of Carbon (Σ New Prod) Obtained by Multiplying Primary Production Rates by the Corresponding *f* Ratio for the 1°N–16°S Transect Along 150°W

Station	Latitude °S	1% LPD, m	ΣPP, mg C m^{-2} d^{-1}	$\Sigma\rho NO_3$, mg-at N m^{-2} d^{-1}	$\Sigma\rho NH_4$, mg-at N m^{-2} d^{-1}	Σ *f* Ratio	Σ New Prod mg C m^{-2} d^{-1}
				Equatorial			
11	−1	65	990	1.65	9.7	0.145	143.92
10	0	77	1090	1.87	12.54	0.130	141.45
9	1	85	740	1.83	7.05	0.206	152.50
8	2.5	90	860	1.77	8.07	0.180	154.70
7	4	83	700	2.68	9.83	0.214	149.96
12	5	86		2.17	10.72	0.168	
13	5.2	87	610	2.05	8.94	0.187	113.79
14	5.23	88	880	2.27	10.42	0.179	157.42
15	5.27	85	870	2.05	8.94	0.187	
16	5.33	89	870				
6	5.5	nd	797	1.56	8.8	0.151	120.01
				Mesotrophic			
5	7	86		1.6	8.23	0.163	
4	8.5	87	620	0.9	7.54	0.107	66.11
3	10	90	570	1.62	6.94	0.189	107.87
				Oligotrophic			
2	11.5	98	370	0.47	4.38	0.097	35.86
1	13	103	290	0.488	5.5	0.081	23.63
17	16	127		1.58	8.23	0.161	
18	16	130		1.19	10.67	0.100	
19	16	125					
20	16	123	560	1.19	10.67	0.100	56.19
21	16	124	550	0.67	7.62	0.084	46.20

of GF/F filters leads to underestimates of the level of particulate matter [*Altabet*, 1990; *Slawyk and Raimbault*, 1995; *Pujo-Pay et al.*, 1997; *Libby and Wheeler*, 1997]. According to this latter observation, values of PON and POC given in this study as well as those from literature data have to be heightened by a factor of 1.5–2.

The distribution of hydrological and biological parameters clearly showed that the properties in terms of biomass varied much less than might be expected from nutrient distributions. However, on the basis of physical and chemical characteristics, three regions could be distinguished along the transect (Table 1). The first region is the oligotrophic region beyond 10°S, characterized by warm, high-salinity, and nitrate poor waters and a euphotic layer >100 m. In this region, areal contents were <100 μg-at m^{-2} and 25 mg m^{-2} for nitrate and chlorophyll, respectively. This area was also characterized by a low N/Si/P ratio, indicating a deficit in nitrogen with respect to the Redfield ratio. The second region is the equatorial region between 1°N and 6°S, where nitrate concentrations in surface waters were >2 μg-at L^{-1} and salinity was <35.5 PSU. Integrated values for nitrate and chlorophyll ranged from 400 to 700 mg-at m^{-2} and from 30 to 40 mg m^{-2}, respectively; the euphotic zone was <90 m thick. This region was characterized by a high NO_3/Si ratio, suggesting a deficit in silicate. The third region is the mesotrophic region between 6° and 10°S where surface nitrate rapidly decreased from 1 μg-at L^{-1} to undetectable values while integrated chlorophyll slightly decreased from 30 to 25 mg m^{-2}. This transitional area was also characterized by undetectable concentrations of ammonium at the surface (Figure 4h), high concentrations of DON, (6.5 μg-at L^{-1}, Figure 4f) in the 0–100 in layer, and decreasing NO_3/Si ratios (Table 1). The northern boundary of the oligotrophic zone was characterized by a salinity front and seemed to be the place of a convergence where surface water downwelled and forwarded to the equator at depths between 100 and 150 m.

3.2. Carbon Fixation and New and Regenerated Production

Primary production in terms of carbon strongly responded to nutrient enrichment of the euphotic zone. Fixation rates were >10 mg C m^{-3} d^{-1} (Figure 5d) in the equatorial zone where nitrate appeared close to the surface. Surface fixation rates ranged between 5 and 10 mg C m^{-3} d^{-1} in the mesotrophic region and were <4 mg C m^{-3} d^{-1} in the oligotrophic area, except at 16°S where five successive profiles gave a mean daily productivity of 5.13 ± 0.80 mg C m^{-3} d^{-1}. In this latter region, significant ^{14}C assimilation (>2 mg C m^{-3} d^{-1}) was measured far below the euphotic zone, until 140 m, while in the other sectors, photosynthetic activity stopped at ~1% LPD (~100 m). This deep primary production explained the small geographical changes in integrated production rates which ranged from 300–500 mg C m^{-2} d^{-1} in the south to 800–1000 mg C m^{-2} d^{-1} near the equator (Table 2). New (ρNO_3) and regenerated (ρNH_4) production rates were also highest in the surface nutrient-enriched area (Figures 5e and 5f). Nitrate uptake was more light-dependent than ammonium uptake, and rates were not significantly different from zero (<0.5 ng-at L^{-1} d^{-1}) below the euphotic zone, except at 13° and 16°S where ρNO_3 reached 4 ng-at L^{-1} d^{-1} in the DCM at 140 m depth. Regenerated production was significant below the 1% LPD (>40 ng-at L^{-1} d^{-1}) at all stations. Values for ρNH_4 were always higher than for ρNO_3 over the entire region, with maximal values occurring in the vicinity of the equator. However, at the equator, general high nutrient availability enhancement of ρNH_4 (by a factor of 3) was not as pronounced as enhancement

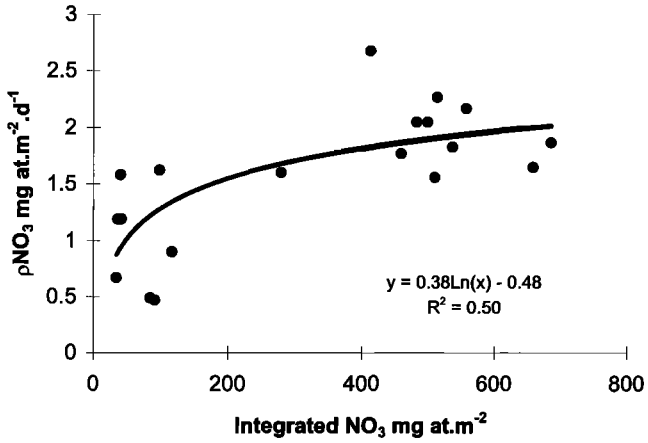

Figure 7. Relationship between the integrated nitrate concentration and the integrated nitrate uptake (ρNO_3) along the 150°W transect between 16°S and 1°N.

of ρNO_3 (by a factor 5). Integrated values of ρNH_4 showed no obvious latitudinal trend and could not be related to integrated values of ammonium concentration (Table 2). It should be remembered that ammonium uptake measured in the oligotrophic region could be overestimated because of the perturbation effect of the tracer addition. In contrast, a positive relationship was found between integrated ρNO_3 and nitrate concentration (Figure 7). Although integrated nitrate concentrations increased by a factor of 17 from the oligotrophic to the equatorial zone (Table 1), integrated new production rates increased only twofold to threefold (Table 2). In the equatorial region, ρNO_3 remained constant (2 mg-at m^{-2} d^{-1}) in spite of the significant increase of nitrate. Exterior to the equatorial zone, nitrate uptake was also poorly related to nitrate. The lack of a good relationship between nitrate concentration and ρNO_3 could explain the poor performance of models that use this relationship in the equatorial Pacific region.

3.3. Nitrogen Regeneration

Ammonium regeneration rates also showed important regional variations (Figure 5g). Regeneration was very active in surface waters around the equator with rates >100 ng-at L^{-1} d^{-1} and between 1° and 6°S with rates >60 ng-at L^{-1} d^{-1}. In the mesotrophic zone, surface values decreased down to 40 ng-at L^{-1} d^{-1}, but higher rates (>50 ng-at L^{-1} d^{-1}) were found at ~100 depth, associated with a subsurface maximum of ammonium. Ammonium regeneration was very low in surface waters of the oligotrophic zone (<20 ng-at L^{-1} d^{-1}) but showed an important subsurface maximum between 10° and 13°S associated with high ammonium concentrations (Figure 4g). At the most oligotrophic station (16°S), ammonium regeneration was low and more or less homogeneous over the water column (5–10 ng-at L^{-1} d^{-1}). Nitrification rates at the oligotrophic site were <5 ng-at L^{-1} d^{-1} in the surface layer but reached values >10 ng-at L^{-1} d^{-1} at depth (Figure 8). In the mesotrophic and upwelling area, nitrification rates reached 40 ng-at L^{-1} d^{-1}. The upwelling area was characterized by high nitrification rates in the whole upper layer, indicating that 20%–100% of nitrate uptake (new production) could be sustained by in situ nitrate regeneration.

3.4. The *f* Ratio

Figure 5h shows the distribution of the *f* ratio, calculated from daily rates of new production and regenerated production which were both corrected for isotope dilution (see section 2). There is a general decrease in *f* with depth due to the greater dependence of nitrate uptake on irradiance than on ammonium uptake. The geographical variation of the ratio is closely related to the distribution of nitrate concentration and nitrate uptake. Values of *f* increased from 16°S (<0.10) to the equatorial region (>0.30) but always rapidly decreased with depth. Values were generally <0.02 below 80 m except at 13° and 16°S where high nitrate uptake rates found in the DCM (below the 1% LPD) led to a ratio >0.15 at a depth >100 m. Values of integrated new and regenerated production as well as of *f* ratios given in Table 2 are consistent with the physical and chemical features of the three areas previously defined. The highest uptake rates were found in the equatorial region where *f* ranged from 0.15 to 0.21. In the mesotrophic region, uptake rates were somewhat lower, and *f* ranged from 0.11 to 0.19. The integrated *f* ratio was used to calculate new production from ^{14}C fixation rates (Table 2). New production appeared to be elevated in the equatorial zone (142 ± 16 mg C m^{-2} d^{-1}), was lower in the mesotrophic region (90 ± 29 mg C m^{-2} d^{-1}),

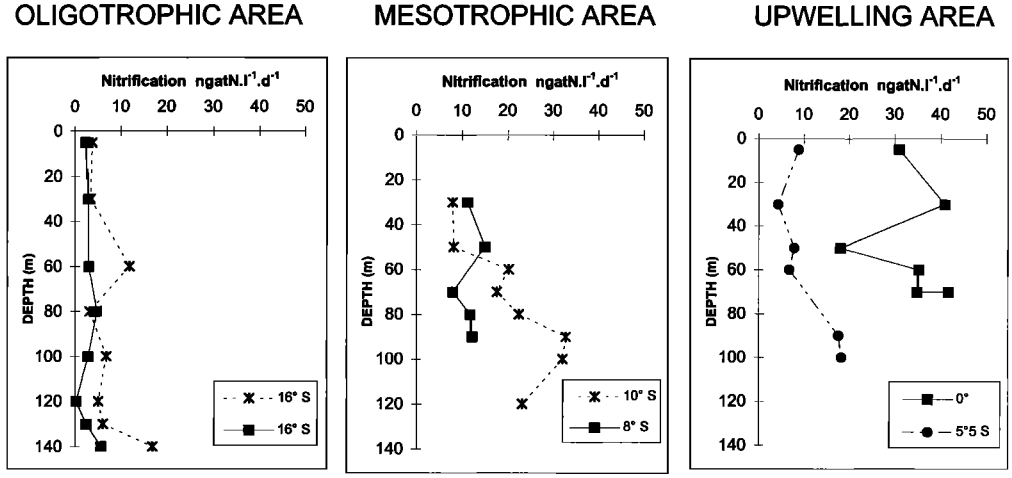

Figure 8. Profiles of ammonium oxidation (nitrification in ng-at L^{-1} d^{-1}) versus depth obtained from the three distinguished regions (see text).

and was lowest in the oligotrophic zone (40.5 ± 14 mg C m^{-2} d^{-1}). Mean total carbon fixation was compared with mean total nitrogen production ($\rho NO_3 + \rho NH_4$) in terms of atomic ρ_C/ρ_N ratio (Figure 9). Values of ρ_C/ρ_N ratios for the equatorial and mesotrophic zones (4 to 7.7 and 5.5, respectively) were close to the Redfield ratio. In the oligotrophic zone the ρ_C/ρ_N ratio was <5. This low ratio may be partly explained by an overestimation of nitrogen uptake in the upper nutrient-depleted layer, where ^{15}N tracer additions, even at nanomolar levels, might have led to an artificial increase in uptake rates. In contrast, the mean C/N composition ratio in seston along the transect was 7.8 ± 1.33 and agreed well with the Redfield ratio.

3.5. Export of Particulate Matter

Fluxes of PM, POC, and PON obtained from experiments with sediment traps are given in Figure 10. All fluxes depicted major latitudinal variations. Maximal fluxes were found in the equatorial region until 4°S, followed by a regular decrease until 10°S. Fluxes in the southern area were very low and showed no significant geographical trend. Spatial patterns in vertical fluxes of POC and PON were similar to those observed for total mass fluxes (PM). The C/N atomic ratio of the flux material was always higher than in the suspended material (Figure 9), increasing from 8–10 in the equatorial region to 10–14 in the oligotrophic area. This latter pattern suggests that marked losses in N occurred in the particles, while comparatively large amounts of C remained associated with particles. This is consistent with the finding that nitrogen is lost more rapidly than carbon from sinking particles [*Knauer et al.*, 1979; *Lohrenz et al.*, 1992]. To provide information on the proportion of total primary production leaving the euphotic zone in the form of sinking particles, we calculated export ratios of carbon (e_{POC} = POC_{flux}/PP) and nitrogen (e_{PON} = PON_{flux}/N uptake) according to *Murray et al.* [1989]. Both e_{POC} and e_{PON} varied along the transect (Figure 11) with the highest values occurring in the equatorial region, thus indicating a positive relationship between export, total primary production, and nitrate availability. Between 16° and 6°S both e_{POC} and e_{PON} values were very low and similar, indicating that only 1%–3% of nitrogen and carbon assimilated by phytoplankton left the euphotic zone in the form of sinking particles. In the equatorial region, rates of export increased to 8%–10% for carbon but only to 6%–8% for nitrogen, suggesting a different fate for carbon and nitrogen.

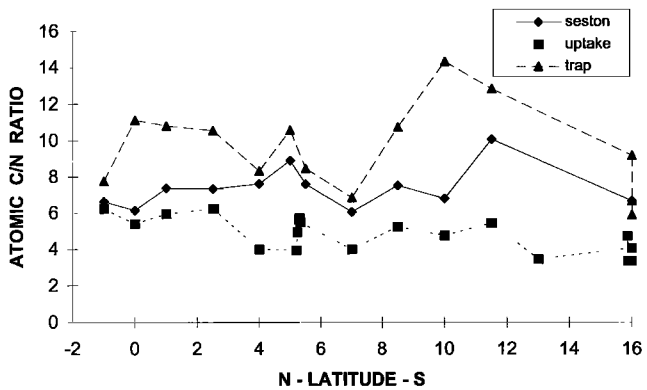

Figure 9. Latitudinal variation of the atomic C/N ratio in suspended materials (seston), trap-collected materials (trap), and from the ^{14}C and ^{15}N uptake experiments (uptake). All ratios are from integrated (0–150 m) values. Results from three repeating stations conducted at 16°S are given.

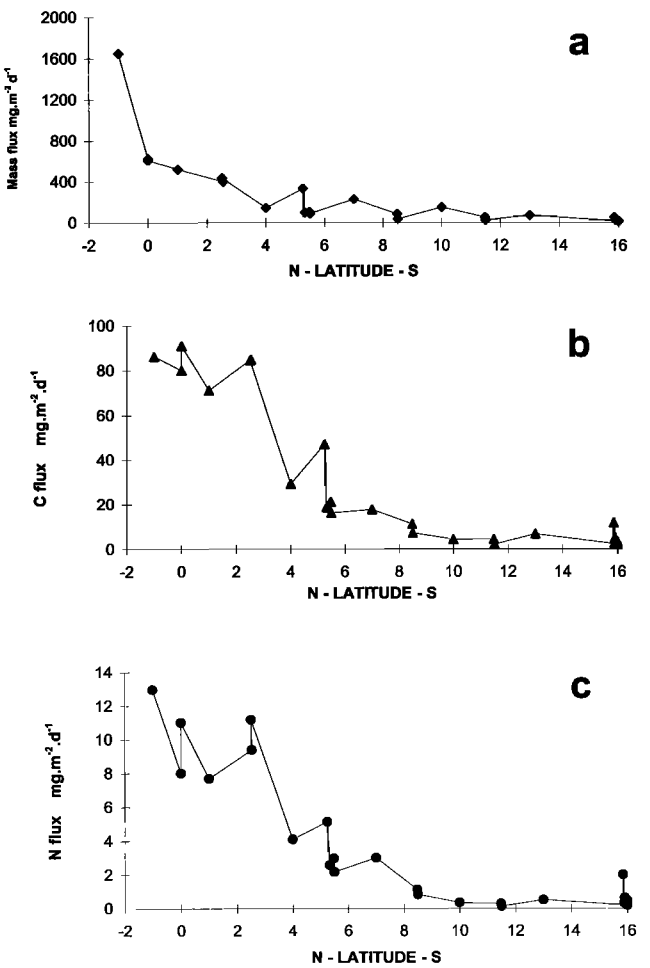

Figure 10. Latitudinal variation of downward flux of (a) particulate matter (mass flux), (b) particulate organic carbon (carbon flux), and (c) particulate organic nitrogen (nitrogen flux). Results from three repetitive stations conducted at 16°S are given.

3.6. Discussion

3.6.1. New versus export production: Impact of DOM in improving C and N budgets. The period from 1991 to 1994 corresponded to a long-lived warm anomaly in the equatorial

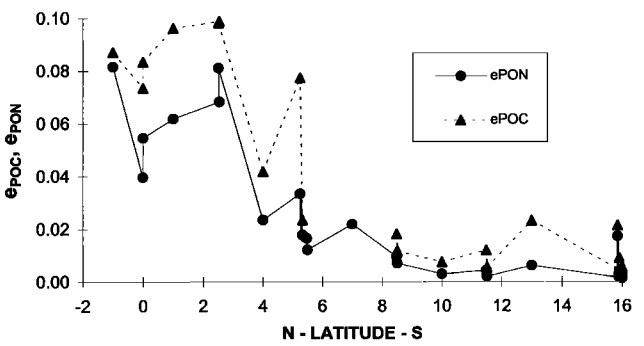

Figure 11. Latitudinal variation of the export ratio in terms of carbon (e_{POC}) and nitrogen (e_{PON}).

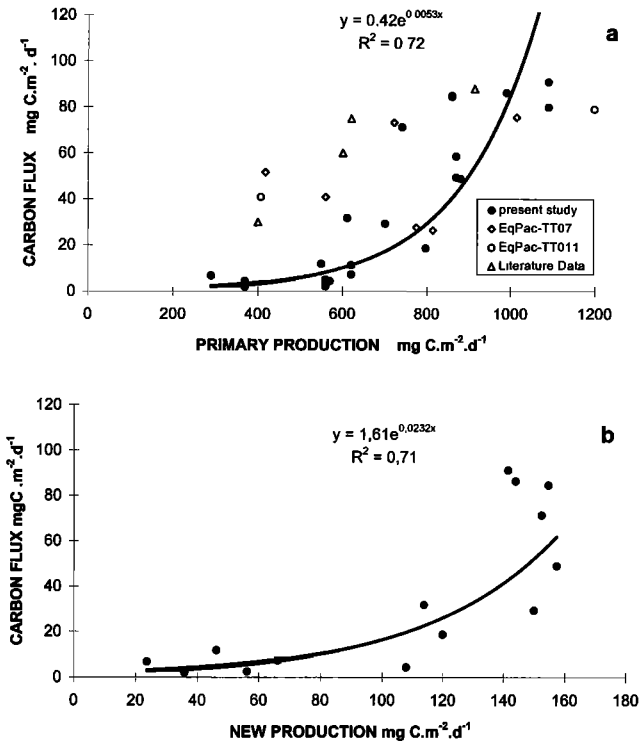

Figure 12. Plot of carbon flux (a) versus primary production and (b) versus new production calculated by multiplying primary production by the f ratio. TT011 and TT007 data are from *Murray et al.* [1996]. Others literature data are from *Chavez et al.* [1996], *Buesseler et al.* [1995], *Betzer et al.* [1984], and *Luo et al.* [1995]. The exponential relationships are calculated from data of this study (solid symbols).

Pacific with two El Niño events in 1991–1992 [*Kessler and McPhaden*, 1995]. Hydrological conditions prevailing during November 1994 were quite similar to those observed in spring 1992 by *Murray et al.* [1995] and typical of a moderate El Niño event, with surface temperatures 2°C higher than the annual mean and nitrate surface concentrations about half of average values [*Chavez et al.*, 1996]. In spite of these warm conditions, primary production (total and new production) in terms of carbon were as high as those observed during normal upwelling conditions. Mean values for total carbon fixation at the equator (950 mg C m^{-2} d^{-1}) were ~2 times higher than values from southern oligotrophic waters (440 mg C m^{-2} d^{-1}) beyond 10°S. These production rates are close to those observed at 135°W in the equatorial zone (1°N–1°S) as well as in the southern oligotrophic region (14°S) during March 1988, 1005 and 456 mg C m^{-2} d^{-1} respectively [*Peña et al.*, 1992], and to those found following the 1992 El Niño event during the EqPac cruises (1000–1500 mg C m^{-2} d^{-1} at the equator and 324–372 mg C m^{-2} d^{-1} at 12°S [*Barber et al.*, 1996]). New production rates near the equator (between 0 and 5°S) were ~140 mg C m^{-2} d^{-1} and were close to the value of 113 mg C m^{-2} d^{-1} found at 150°W during the WEC88 cruise [*Dugdale et al.*, 1992]. Our rates comprised those measured under El Niño (50 mg C m^{-2} d^{-1}) and non–El Niño (222 mg C m^{-2} d^{-1}) conditions [*McCarthy et al.*, 1996]. However, our nitrate uptake rates measured poleward to 5°S were much higher (by a factor of 2–3) than those found in 1988 by *Dugdale et al.* [1992]. In fact, in 1988 the area of high nitrate and ammonium uptake was limited to a narrow band near the equator, while during the present work, high productivity rates occurred far to the south (until 7°S).

There was a good agreement between new production (in terms of carbon) computed from direct measurements of nitrate uptake and the Redfield ratio ($\rho_{NO3} \times 6.6$) and new production obtained from ^{14}C fixation rates multiplied by the independently estimated f ratio. This seems to demonstrate that new production in terms of carbon in the equatorial Pacific may be estimated with confidence from measurements with the ^{15}N tracer and used for modeling purposes. Values of f found in this study (0.08–0.30) agree well with those noted by *Dugdale et al.* [1992] and *McCarthy et al.* [1996] but were much lower (twofold to fivefold) than those estimated from models of *Eppley and Peterson* [1979] and *Platt and Harrison* [1985]. This latter discrepancy seems to indicate that the equatorial upwelling, in spite of its nitrate rich waters, is distinct from coastal upwellings to which the latter f ratio models apply.

According to *Eppley and Peterson* [1979] the f ratio is defined as the fraction of total production (new production) that must leave the euphotic zone to balance the input of new inorganic nitrogen. However, our data show that the amount of carbon and nitrogen produced in the euphotic zone (new production) is always greater than the corresponding amount recovered in sediment traps. Export ratios (e_{POC} and e_{PON}, Figure 11) were significantly lower than f ratios, indicating that only a small part of new production is exported through sinking particles especially in the mesotrophic and oligotrophic area where export represented <10% of new production. However, we obtained a relationship between primary production and carbon flux at the base of the euphotic zone (Figure 12). Figure 12a, which includes data from literature, shows that our measurements of particulate carbon flux are comparable with direct measurements using other types of sediment traps and with indirect measurements using ^{234}Th [*Buesseler et al.*, 1995; *Murray et al.*, 1996] in areas where primary production is >600 mg C m^{-2} d^{-1}. For example, C and N particle fluxes measured at the equator (70–80 and 8–10 mg m^{-2} d^{-1}, respectively) are close to estimations of *Betzer et al.* [1984] obtained from sediment traps deployed at 900 m and to those of *Murray et al.* [1989] from the eastern Pacific. Along 140°W, *Buesseler et al.* [1995] and *Murray et al.* [1996] observed a particulate carbon export from the upper 100 m of ~25 mg C m^{-2} d^{-1} (at ~4°S) and an equatorial peak of 60 mg C m^{-2} d^{-1}, which are very close to our estimations. However, our sinking fluxes measured in less productive waters (<600 mg C m^{-2} d^{-1}) were much lower than those given for the same region by *Murray et al.* [1996], who placed their sediment traps at shallower depths (120 versus 200 m for ours). This difference between the collecting depth of the traps may explain the discrepancies between sinking rates since particle flux is highly dependent on sampling depth and decreases greatly between 100 and 200 m [*Luo et al.*, 1995]. On the other hand, our rates are consistent with those found in the oligotrophic Sargasso Sea [*Lohrenz et al.*, 1992]. Vertical carbon flux is exponentially related to new production (Figure 12b). This exponential model predicts that a threefold increase in new production, which occurs when moving from oligotrophic into equatorial waters, would result in a tenfold increase in the downward flux of organic material. The model also confirms differences in the fate of particulate organic matter; that is, particles are more strongly retained in the euphotic layer of unproductive oligotrophic areas than in the euphotic layer of productive upwelling areas [*Lohrenz et al.*, 1992].

Several reasons are evoked to explain the discrepancy between rates of new production measured with isotopic tracers and export production obtained from sediment traps. First, the discrepancy may be a result of a methodological bias since particles were collected 50 m below the euphotic zone. Second, the discrepancy may be caused by horizontal advection which explains the lack of agreement between new production and export measured at the same geographical location. The equatorial region is characterized by an active current system with the south equatorial current flowing to the west and the intense equatorial undercurrent flowing to the east. Therefore particulate materials produced in the upwelling area may be rapidly advected away and consequently would not fall strictly vertically.

Another possible cause of the discrepancy is that the f ratio used to calculate new production could be overestimated. Historically, regenerated production was measured exclusively using ammonium uptake. Dissolved organic nitrogen found in relatively high concentrations in marine waters, resulting from zooplankton excretion, bacterial remineralization, or direct release by phytoplankton cells, may represent a significant source of nitrogen for phytoplankton [*Antia et al.*, 1991; *Bronk et al.*, 1993]. More precise estimations of the f ratio would need measurements of DON uptake, especially urea. Inspecting data from literature, *Wafar et al.* [1995] have demonstrated that exclusion of urea uptake from the calculation overestimated the f ratio in upwelling and oceanic regions from 16% to 42%. Applying this correction to our data led to lower values for the f ratio in the equatorial (0.15) and the oligotrophic (<0.05) region. New production rates between 0 and 3°S calculated with these corrected values agreed rather well with sinking rates of particles, but discrepancies (up to 80%) between both rates still existed in the southern region. Failure to account for nitrification as a source of in situ regenerated nitrate could lead to a overestimation of the f ratio. As previously found by *Ward* [1985] and *Gentilhomme and Raimbault* [1994], nitrification rates found at the base of the euphotic zone were high enough to fuel the daily nitrate demand by phytoplankton. This led the latter authors to conclude that a great part of nitrate uptake was regenerated production rather than new production.

For many authors a further explanation for the disagreement between rates of new production and export production is that the horizontal advection or vertical mixing of dissolved organic matter (DOM) can exceed fluxes of sinking particles and thus appear as a major fate of new production [*Copin-Montégut and Avril*, 1993; *Peltzer and Hayward*, 1996]. *Toggweiler* [1989] reported that balance solely between upward nutrient flux and sinking particles in a three-dimensional modeling study led to overincreasing nutrient concentrations and particles fluxes. The most realistic simulations were obtained when half of the new production due to upwelled nutrient went into a pool of organic compounds. The release of DON in short-term incubation experiments has been reported for several types of marine waters [*Bronk et al.*, 1994; *Slawyk and Raimbault*, 1995]. Work on DI^{15}N losses performed during this cruise [*Slawyk et al.*, 1999] indicated that only a small fraction of $^{15}N\text{-}NO_3$ taken up (2%–10% in mesotrophic and oligotrophic regions) was ultimately found in the extracellular DON pool at the end of incubation. The percentage of nitrogen lost by phytoplankton as DON (DON release) was in fact higher than these values (by 1 order of magnitude) as a result of the dilution of the tracer nitrogen during incorporation in the initially unlabeled planktonic material [*Slawyk et al.*, 1999]. Consequently, the DON release via excretion, cell lysis, or sloppy feeding might represent at least ~20–100% of the new production. Moreover, the simultaneous decrease in nitrate and increase in DON (Figure 6), as surface water moves away from the equator, may be indicative of (1) net production of DON, (2) DON export as water moves poleward, and (3) DON accumulation in the convergence zone (Figure 4f). The meridional decrease in nitrate (from 2 to 0.24 = 1.76 μg-at L^{-1}) and increase of DON (from 5.7 to 6.9 = 1.20 μg-at L^{-1}) from the equatorial zone to the mesotrophic zone revealed that 68% of the nitrate that disappeared was accumulated as DON, a value close to the 81% estimate of *Libby and Wheeler* [1997]. Then we can hypothesize that a large fraction of inorganic nitrogen consumed in the equatorial zone is recovered in the dissolved organic pool in the mesotrophic area and transported meridionally away from the equator until 11°–13°S. Adding this DON production to the particulate matter flux would roughly balance the nitrogen budget in the euphotic zone. Similar data concerning DOC release are not yet available. However, from the likeness of the ρ_C/ρ_N and C/N ratios we may suggest that the ratio of release to export is the same for DOC and DON. This assumption is strengthened by the fact that a large increase of DOC in the upper layer occurred between 6° and 10°S [*Peltzer and Hayward*, 1996]. In this case, lateral advection of DOC would provide an important sink for assimilated carbon. One should emphasize that the DON accumulation as well as the high DOC content observed by *Peltzer and Hayward* [1996] occurred between 5° and 10°S, i.e., in the convergence zone. According to the three-dimensional circulation model of *Toggweiler and Carson* [1995] the surface convergence takes place on either side of the equator and results in downwelling of the surface water. This hydrodynamical feature can explain the large extension in depth of the DON rich waters (>6.5 μg-at L^{-1} at 100 m, Figure 4f). At depth, DON may be remineralized as concluded from active ammonium regeneration (>100 ng-at L^{-1} d^{-1}) and ammonium accumulation found in this region (Figure 4h). Near-surface maxima of heterotrophic bacteria have been found centered around the convergence zone [*Landry et al.*, 1996] depicting this zone as an active region of remineralization. *Toggweiler and Carson*'s [1995] model suggests that downwelled water recirculates in the equatorial undercurrent at depths of 50–150 m back toward the equator. In our case, inorganic nitrogen resulting from DON remineralization could have been, in part, upwelled and thus have reached again the euphotic zone. This cell circulation between the equatorial upwelling, the poleward convergence, and the downwelling may efficiently maintain nitrogen in the system if the upwelling source is not deeper than 100–150 m. The only loss of organic matter from this system would be due to sinking particles which appear as a very low fraction of new production.

3.6.2. Does the equatorial cell circulation explain the HNLC situation? One of the remaining questions concerns why the phytoplankton biomass and productivity in the equatorial Pacific is not as high as the nitrate level could potentially support. Why is the equatorial Pacific not greener [*Barber*, 1992]? The small variations in chlorophyll compared to the large variations in the physical environment argue for a chemical and/or biological factor regulating chlorophyll concentration in the equatorial Pacific. While possible explanations, such as grazing [*Walsh*, 1976] and nutrient limitation by macronutrients or micronutrients, have been well discussed in literature, iron is actually the most likely candidate [*Lindley et al.*, 1995; *Martin et al.*, 1994; *Chavez and Smith*, 1995]. In our case the fact that the f ratio was lower than expected from nitrate

concentration might be explained by a greater effect of iron deficiency on nitrate uptake than on ammonium uptake. Several experiments of iron enrichment have recently demonstrated that only diatoms are stimulated by artificial iron addition [*Fitzwater et al.*, 1996; *Zettler et al.*, 1996]. From this observation, one may conclude that iron deficiency leads to the maintenance of a population trapped in a small-sized, low-sinking rate group of species that encourage grazing or the functioning of a microbial loop which in turn holds the residence time of the cells to about a day [*Cullen et al.*, 1992; *Wilkerson and Dugdale*, 1992]. *Peduzzi and Herndl* [1992] have shown that zooplankton grazing on phytoplankton fuels the microbial loop through the release of labile dissolved organic matter. The levels of ammonium regeneration measured in this study tend to confirm this hypothesis. At the equator, although ammonium concentrations were low (not high enough to inhibit nitrate uptake), ammonium regeneration (>150 ng-at L^{-1} d^{-1}) supplied enough nitrogen to sustain high phytoplanktonic growth rates. Considering a chlorophyll/nitrogen ratio of 1 for this region [*Eppley et al.*, 1992], the daily growth rate of regenerated ammonium was ~0.5–0.7 d^{-1}. However, we wish to point out the possible role played by new silicate in limiting primary productivity in the equatorial region, keeping in mind that "no single factor can be said to control phytoplankton to the exclusion to others" [*Chisholm and Morel*, 1991, Introduction]. We observed anomalies in the nitrogen/silicate ratio in surface waters between 0 and 5°S, suggesting a possible silicate limitation of diatom growth as noted in coastal upwelling [*Dugdale et al.*, 1995; *Copin-Montégut and Raimbault*, 1994] as well as in the equatorial Pacific divergence [*Dugdale and Wilkerson*, 1998]. Diatom biomass decreased to "background" levels at latitude 5°S [*Bidigare and Ondrusek*, 1996], and *Chavez* [1987] concluded that the occurrence of blooming is unlikely in the equatorial Pacific because of the absence of chain-forming diatoms. *Bender and McPhaden* [1990] have reported similar high nitrate/silicate ratios (>6.6) near the equator at 140°W in 1988 and suggested that this anomalous nutrient distribution resulted from rapid silicate removal by a transient biological event.

With the help of our chemical and biological data and recent data from literature we can propose a schematic picture of the functioning of the ecosystem of the central equatorial Pacific upwelling. Low utilization of available nitrate was likely the consequence of a grazing effect by microzooplankton as well as by mesozooplankton. Grazing would reduce the autotrophic biomass and absolute inorganic nitrogen consumption and also increase the availability of DON which could in turn stimulate the ammonium regeneration via heterotrophic bacteria [*Kirchman et al.*, 1989]. Since ammonium is generally the preferred form of nitrogen used by phytoplankton, especially by small-sized species, its availability may be an important regulator of new production in this nitrate rich environment. Thus the equatorial system is locked into a strong grazing loop dominated by small organisms <10μm [*Peña et al.*, 1991; *Chavez*, 1989], with virtually everyday's production consumed within the same period [*Cullen et al.*, 1992]. During some periods of intense upwelling, at times when the equatorial thermocline shoals and mixed layer nutrient concentration rises, diatom blooms might occur, leading to transient high new production associated with high silicate [*Bender and McPhaden*, 1990] and maybe iron consumption. While nitrogen is efficiently recycled via DON release and ammonium regeneration, a great part of silicate and maybe also of iron might leave the euphotic zone via sinking diatoms and might not be sufficiently remineralized. Evidence for rapid losses via vertical transport was apparent from deep sediment trap fluxes measured by *Honjo et al.* [1995] during the EqPac study in January 1992. Silicate-depleted waters could have entered into the "conveyor belt" meridional circulation. Consequently, when the perturbed system returns to equilibrium, surface waters at the equator, upwelled from low depths and in part fueled by surface water from the convergence, where nitrogen and maybe a great part of phosphorus and carbon are remineralized, have lost most of their silicate. This loss of particulate silicate and the recycling of only nitrogen via biological and physical processes may explain the deficiency in silicate observed in the upwelled water at the equator during El Niño events. Equatorial regions characterized by low silicate concentrations, i.e., NO_3/Si ratios $\gg 1$, and by high levels of ammonium and in situ nitrate regeneration can be qualified as a new Si-limited system [*Ku et al.*, 1995] where new production and export were mostly controlled by silicate. More data on nitrification, especially from the equatorial undercurrent, are required to fully elucidate the equatorial nitrogen cycle, while data on solid biogenic silica (opal) and iron in sediment particles are needed to understand better the origin of these macronutrient and micronutrient deficiencies. Therefore, in spite of significantly high new production at the equator compared to the oligotrophic system the net biological effect of the equatorial upwelling in the CO_2 export should be very weak but could be activated by a significant transient supply of silicate (and iron) forced by ocean circulation (strong shoaling of thermocline), thus initiating blooms of large sinking cells like diatoms.

Acknowledgments. The Oligotrophie en Pacifique (OLIPAC) cruise was a contribution to the JGOFS-France program in the equatorial Pacific and was included in the Etude des Processus dans l'Océan Pacifique Equatorial (EPOPE) program with the FLUx dans l'ouest du PACifique equatorial (FLUPAC) cruise (October 1994) mainly devoted to the study of the primary productivity along 165°E and along the equator between 165°E and 150°W. Funds came from the French organizations IFREMER, INSU, and by ORSTOM. We are grateful to the crew of the R/V *L'Atalante* for efficient help during the cruise. We wish to thank D. Taillez and C. Bournot for CTD data and for collecting samples of sediment traps and A. Morel and S. Maritorena for providing light data. We thank M. C. Bonin for drawing figures and contributing data from literature. The authors also thank the two anonymous referees, who helped to improve the final version of the manuscript.

References

Allen, C. B., J. Kanda, and E. A. Laws, New production and photosynthetic rates within and outside a cyclonic mesoscale eddy in the North Pacific subtropical gyre, *Deep Sea Res., Part II, 43*, 917–936, 1996.

Altabet, M. A., Organic C, N and stable isotopic composition of particulate matter collected on glass-fiber and aluminium oxide filters, *Limnol. Oceanogr., 35*, 902–909, 1990.

Antia, N. J., P. J. Harrison, and L. Oliveira, The role of dissolved organic matter in phytoplankton nutrition, cell biology and ecology, *Phycologia, 30*, 1–89, 1991.

Barber, R. T., Introduction to the WCE88 cruise: An investigation into why the equator is not greener, *J. Geophys. Res., 97*, 609–610, 1992.

Barber, R. T., M. P. Sanderson, S. T. Lindley, F. Chay, C. C. Trees, D. G. Foley, and F. P. Chavez, Primary productivity and its regulation in the equatorial Pacific during and following the 1991–1992, El Niño, *Deep Sea Res., Part II, 43*, 933–969, 1996.

Bender, M. L., and M. J. McPhaden, Anomalous nutrient distribution in the equatorial Pacific in April 80: Evidence for rapid biological uptake, *Deep Sea Res., Part A, 37*, 1075–1084, 1990.

Betzer, P. R., W. J. Showers, E. A. Laws, C. D. Wenn, G. R. Di Tullio, and P. M. Kroopnick, Primary productivity and particle fluxes on a transect of the equator at 153°W in the Pacific Ocean, *Deep Sea Res., Part A, 31*, 1–11, 1984.

Bidigare, R. R., and M. E. Ondrusek, Spatial and temporal variability of phytoplankton pigment distributions in the central equatorial Pacific Ocean, *Deep Sea Res., Part II, 43*, 809–833, 1996.

Bronk, D., and P. M. Glibert, Application of a ^{15}N tracer method to the study of dissolved organic nitrogen uptake during spring and summer in Chesapeake Bay, *Mar. Biol., 115*, 501–508, 1993.

Bronk, D. A., P. M. Glibert, and B. B. Ward, Nitrogen uptake, dissolved organic nitrogen release and new production, *Science, 265*, 1843–1846, 1994.

Buesseler, K. O., J. A. Andrews, M. C. Hartman, R. Belastock, and F. Chai, Regional estimates of the export flux of particulate organic carbon derived from thorium-243 during the JGOFS EqPac program, *Deep Sea Res., Part II, 42*, 777–804, 1995.

Carr, M.-E., N. S. Oakey, B. Jones, and M. R. Lewis, Hydrographic patterns and vertical mixing in the equatorial Pacific along 150°W, *J. Geophys. Res., 97*, 611–626, 1992.

Chavez, F. P., Size distribution of phytoplankton in the central and eastern tropical Pacific, *Global Biogeochem. Cycles, 3*, 27–35, 1989.

Chavez, F. P., and R. T. Barber, An estimate of new production in the equatorial Pacific, *Deep Sea Res., Part A, 34*, 1229–1243, 1987.

Chavez, F. P., and S. L. Smith, Biological and chemical consequences of open ocean upwelling, in *Upwelling in the Ocean: Modern Processes and Ancient Records*, edited by C. P. Summerhayes et al., pp. 149–170, John Wiley, New York, 1995.

Chavez, F. P., K. R. Buck, S. K. Service, J. Newton, and R. T. Barber, Phytoplankton variability in the central and eastern tropical Pacific, *Deep Sea Res., Part II, 43*, 835–970, 1996.

Chisholm, S. W., and F. M. M. Morel, What controls phytoplankton production in nutrient-rich areas of the open ocean?, *Limnol. Oceanogr., 36*, 1507–1970, 1991.

Copin-Montégut, G., and B. Avril, Vertical distribution and temporal variation of dissolved organic carbon in the north-western Mediterranean Sea, *Deep Sea Res., Part I, 40*, 1963–1972, 1993.

Copin-Montégut, C., and P. Raimbault, The Peruvian upwelling near 15°S in August 1986: Results of continuous measurements of physical and chemical properties between 0 and 200 m depth, *Deep Sea Res., Part I, 41*, 439–467, 1994.

Cullen, J. J., M. R. Lewis, C. O. Davis, and R. T. Barber, Photosynthetic characteristics and estimated growth rates indicate grazing is the proximate control of primary production in the equatorial Pacific, *J. Geophys. Res., 97*, 639–654, 1992.

Deuser, W. G., E. H. Ross, and R. F. Anderson, Seasonality in the supply of sediment to the deep Sargasso Sea, and implications for the rapid transfer of matter to the deep ocean, *Deep Sea Res., Part A, 28*, 495–505, 1981.

Dugdale, R. C., and J. J. Goering, Uptake of new and regenerated forms of nitrogen in primary productivity, *Limnol. Oceanogr., 12*, 196–206, 1967.

Dugdale, R. C., and F. P. Wilkerson, The use of ^{15}N to measure nitrogen uptake in eutrophic oceans, experimental considerations, *Limnol. Oceanogr., 31*, 673–689, 1986.

Dugdale, R. C., and F. P. Wilkerson, Silicate regulation of new production in the equatorial Pacific upwelling, *Nature, 311*, 270–273, 1998.

Dugdale, R. C., F. P. Wilkerson, F. P. Chavez, and R. T. Barber, Estimating new production in the equatorial Pacific at 150°W, *J. Geophys. Res., 97*, 681–686, 1992.

Dugdale, R. C., F. P. Wilkerson, and H. J. Minas, The role of a silicate pump in diving new production, *Deep Sea Res., Part I, 42*, 697–719, 1995.

Eppley, R. W., and B. J. Peterson, Particulate organic matter flux and planktonic new production in the deep ocean, *Nature, 282*, 677–680, 1979.

Eppley, R. W., F. P. Chavez, and T. R. Barber, Standing stocks of particulate carbon and nitrogen in the equatorial Pacific at 150°W, *J. Geophys. Res., 97*, 655–661, 1992.

Fitzwater, S. E., K. H. Coale, R. M. Gordon, K. S. Johnson, and M. E. Ondrusek, Iron deficiency and phytoplankton growth in the equatorial Pacific, *Deep Sea Res., Part II, 43*, 995–1015, 1996.

Fleming, R. H., The composition of plankton and units for reporting population and production, paper presented at Sixth Pacific Science Congress, Sears Foundation, San Francisco, Calif., 1939.

Gentilhomme, V., and P. Raimbault, Absorption et régénération de l'azote dans la zone frontale du courant algérien (Méditerranée ocidentale): Réévaluation de la production nouvelle, *Oceanol. Acta, 17*, 555–562, 1994.

Glibert, P. M., F. Lipschultz, J. J. McCarthy, and M. A. Altabet, Isotope dilution models of uptake and remineralization of ammonium by marine plankton, *Limnol. Oceanogr., 27*, 639–650, 1982.

Harrison, W. G., L. R. Harris, and B. D. Irwin, The kinetics of nitrogen utilization in the oceanic mixed layer: Nitrate and ammonium interactions at nanomolar concentrations, *Limnol. Oceanogr., 41*, 16–32, 1996.

Honjo, S., J. Dymond, R. Collier, and S. J. Manganini, Export production of particles to the interior of the equatorial Pacific Ocean during the 1992 EqPac experiment, *Deep Sea Res., Part II, 42*, 831–870, 1995.

Kessler, W. S., and M. J. McPhaden, The 1991–1993 El Niño in the central Pacific, *Deep Sea Res., Part II, 42*, 295–333, 1995.

Kirchman, D. L., R. G. Keil, and P. A. Wheeler, The effect of amino acids on ammonium utilization and regeneration by heterotrophic bacteria in the subarctic Pacific, *Deep Sea Res., Part A, 36*, 1763–1776, 1989.

Knauer, G. A., J. H. Martin, and K. W. Bruland, Fluxes of particulate carbon, nitrogen and phosphorus in the upper water column of the northeast Pacific, *Deep Sea Res., Part A, 37*, 1121–1134, 1979.

Ku, T. L., S. Luo, M. Kusakabe, and J. K. B. Bishop, ^{228}Ra derived nutrient budgets in the upper equatorial Pacific and the role of "new" silicate in limiting productivity, *Deep Sea Res., Part II, 42*, 479–498, 1995.

Landry, M. R., J. D. Kirshtein, and J. Constantinou, Abundances and distributions of picoplankton populations in the central equatorial Pacific from 12°N to 12°S, 140°W, *Deep Sea Res., Part II, 43*, 871–890, 1996.

Libby, P. S., and P. A. Wheeler, Particulate and dissolved organic nitrogen in the central and eastern equatorial Pacific, *Deep Sea Res., Part I, 44*, 345–361, 1997.

Lindley, S. T., R. R. Bidigare, and R. T. Barber, Phytoplankton photosynthesis parameters along 140°W in the equatorial Pacific, *Deep Sea Res., Part II, 42*, 441–464, 1995.

Lohrenz, S. E., G. A. Knauer, V. L. Asper, M. Tuel, A. F. Michaels, and A. H. Knap, Seasonal variability in primary production and particle flux in the northwestern Sargasso Sea: US JGOFS Bermuda Atlantic Time-Series Study, *Deep Sea Res., Part A, 39*, 1373–1391, 1992.

Luo, S., T. L. Ku, M. Kusakabe, J. K. B. Bishop, and Y. L. Yang, Tracing particle cycling in the upper ocean with ^{230}Th and ^{228}Th: An investigation in the equatorial Pacific along 140°W, *Deep Sea Res., Part II, 42*, 805–830, 1995.

Martin, J. H., Glacial-interglacial CO_2 change: The iron hypothesis, *Paleooceanography, 5*, 1–13, 1990.

Martin, J. H., et al., Testing the iron hypothesis in ecosystems of the equatorial Pacific Ocean, *Nature, 371*, 123–129, 1994.

McCarthy, J. J., C. Garside, J. L. Nevins, and R. T. Barber, New production along 140°W in the equatorial Pacific during and after the 1992 El Niño event, *Deep Sea Res., Part II, 43*, 1065–1093, 1996.

Minas, H. J., M. Minas, and T. T. Packard, Productivity in upwelling areas deduced from hydrographic and chemical fields, *Limnol. Oceanogr., 31*, 1182–1206, 1986.

Murray, J. W., J. Downs, S. Strom, C. L. Wei, and H. Jannasch, Nutrient assimilation, export production and ^{234}Th scavenging in the eastern equatorial Pacific, *Deep Sea Res., Part A, 36*, 1471–1489, 1989.

Murray, J. W., R. T. Barber, M. R. Roman, M. P. Bacon, and R. A. Feely, Physical and biological controls on carbon cycling in the equatorial Pacific, *Science, 266*, 58–65, 1994.

Murray, J. W., E. Johnson, and C. Garside, A U.S. JGOFS process study in the equatorial Pacific (EqPac): Introduction, *Deep Sea Res., Part II, 42*, 275–293, 1995.

Murray, J. W., J. Young, J. Newton, J. Dunne, T. Chapin, B. Paul, and J. J. McCarthy, Export flux of particulate organic carbon from the central equatorial Pacific determined using a combined drifting trap-^{234}Th approach, *Deep Sea Res., Part II, 43*, 1095–1132, 1996.

Peduzzi, P., and G. J. Herndl, Zooplankton activity fueling the microbial loop-differential growth response of bacteria from oligotrophic and eutrophic waters, *Limnol. Oceanogr., 37*, 1087–1092, 1992.

Peltzer, E. T., and N. A. Hayward, Spatial and temporal variability of

total organic carbon along 140°W in the equatorial Pacific Ocean in 1992, *Deep Sea Res., 43, Part II, 43*, 1155–1180, 1996.

Peña, M. A., M. R. Lewis, and W. G. Harrison, Particulate organic matter and chlorophyll in the surface layer of the equatorial Pacific Ocean along 135°W, *Mar. Ecol. Prog. Ser., 72*, 179–188, 1991.

Peña, M. A., M. R. Lewis, and W. G. Harrison, Primary productivity and size structure of phytoplankton biomass on a transect of the equator at 135°W in the Pacific Ocean, *Deep Sea Res., Part A, 37*, 295–315, 1992a.

Peña, M. A., W. G. Harrison, and M. R. Lewis, New production in the central equatorial Pacific, *Mar. Ecol. Prog. Ser., 80*, 265–274, 1992b.

Platt, T. T., and W. G. Harrison, Biogenic fluxes of carbon and nitrogen in the ocean, *Nature, 318*, 55–58, 1985.

Preston, T., and N. J. P. Owens, Interfacing an elemental analyzer with an isotope ratio mass spectrometer: The potential for fully automated total nitrogen and nitrogen-15 analysis, *Analyst, 108*, 971–977, 1983.

Pujo-Pay, M., and P. Raimbault, Improvement of the wet-oxidation procedure for the simultaneous determination of particulate organic nitrogen and phosphorus collected on filters, *Mar. Ecol. Prog. Ser., 105*, 203–207, 1994.

Pujo-Pay, M., P. Raimbault, and P. Conan, Underestimation of particulate nitrogen concentrations in the open ocean by the use of GF/F filters, *C.R. Acad Sci., Sec. II, 324*, 401–407, 1997.

Raimbault, P., I. Taupier-Letage, and M. Rodier, Vertical size distribution of phytoplankton in the western Mediterranean Sea during early summer, *Mar. Ecol. Prog. Ser., 45*, 153–158, 1988.

Raimbault P., G. Slawyk, B. Coste, and J. Fry, Feasibility of using an automated procedure for the determination of seawater nitrate in the 0–100 nM range: Examples from field and cultures, *Mar. Biol., 104*, 347–351, 1990.

Slawyk, G., and P. Raimbault, A simple procedure for simultaneous recovery of dissolved inorganic and organic nitrogen in ^{15}N-tracer experiments and improving the isotopic mass balance, *Mar. Ecol. Prog. Ser., 124*, 289–299, 1995.

Slawyk, G., P. Raimbault, and N. Garcia, Measuring gross uptake of ^{15}N-labeled nitrogen by marine phytoplankton without particulate matter collection: Evidence of low ^{15}N losses to the dissolved organic nitrogen pool, *Limnol. Oceanogr.*, in press, 1999.

Suess, E., Particulate organic carbon flux in the oceans: Surface productivity and oxygen utilization, *Nature, 288*, 260–263, 1980.

Tans, P., I. Y. Fung, and T. Takahashi, Observational constraints on the global atmospheric CO_2 budget, *Science, 247*, 1431–1438, 1990.

Thomas, W. H., Nutrient inversions in the southeastern tropical Pacific Ocean, *Fish. Bull., 70*, 929–932, 1972.

Thomas, W. H., Anomalous nutrient-chlorophyll interrelationships in the offshore eastern tropical Pacific Ocean, *J. Mar. Res., 37*, 327–335, 1979.

Toggweiler, J. R., Is the downward dissolved organic matter (DOM) flux important in carbon export, in *Productivity of the Ocean: Present and Past*, edited by W. H. Berger et al., pp. 65–84, Wiley-Intersci., New York, 1989.

Toggweiler, J. R., and S. Carson, What are upwelling systems contributing to the ocean's carbon and nutrient budgets? in *Upwelling in the Ocean: Modern Processes and Ancient Records*, edited by C. P. Summerhayes et al., pp. 337–360, John Wiley, New York, 1995.

Tréguer, P., and P. LeCorre, *Manuel d'Analyse Des Sels Nutritifs Dans l'Eau de Mer: Utilisation de l'AutoAnalyser II Technicon*, 2nd ed., Univ. of Bretagne Occidentale, Lab. de Chim. Mar., Brest, France, 1975.

Wafar, M. V. M., P. Le Corre, and S. L'Helguen, *f*-ratios calculated with and without urea uptake in nitrogen uptake by phytoplankton, *Deep Sea Res.*, Part I, *42*, 1669–1674, 1995.

Walsh, J. J., Herbivory as a factor in patterns of nutrient utilization in the sea, *Limnol. Oceanogr., 21*, 1–13, 1976.

Ward, B. B., Light and substrate concentration relationship with marine assimilation and oxidation rates, *Mar. Chem., 16*, 301–316, 1985.

Wilkerson, F. P., and R. C. Dugdale, Measurements of nitrogen productivity in the equatorial Pacific, *J. Geophys. Res., 97*, 669–680, 1992.

Wyrtki, K., and B. Kilonsky, Mean water and current structure during the Hawaii-to-Tahiti shuttle experiment, *J. Phys. Oceanogr., 14*, 242–254, 1984.

Zettler, E. R., R. J. Olson, B. J. Binder, S. W. Chisholm, S. E. Fitzwater, and R. M. Gordon, Iron-enrichment bottle experiments in the equatorial Pacific: Responses of individual phytoplankton cells, *Deep Sea Res., Part II, 43*, 1017–1029, 1996.

B. Boudjellal, Institut des Sciences de la Mer et de l'Aménagement du Littoral, B.P. 54, Sidi Fredj, Staouel: 42321, Algérie.

C. Coatanoan, P. Conan, B. Coste, N. Garcia, T. Moutin, M. Pujo-Pay, P. Raimbault, and G. Slawyk, Laboratoire d'Océanographie et de Biogéochimie (UMR CNRS 6535), Centre d'Océanologie de Marseille, Campus de Luminy, F-13288 Marseille Cedex, France. (raimbault@com.univ-mrs.fr)

(Received September 8, 1997; revised August 10, 1998; accepted August 31, 1998.)